

In Situ Click Chemistry: Enzyme Inhibitors Made to Their Own Specifications

Roman Manetsch,[†] Antoni Krasinski,[†] Zoran Radić,[‡] Jessica Raushel,[†]
Palmer Taylor,[‡] K. Barry Sharpless,[†] and Hartmuth C. Kolb*[†]

Contribution from the Department of Chemistry and the Skaggs Institute for Chemical Biology, The Scripps Research Institute, 10550 North Torrey Pines Road, La Jolla, California 92037, and the Department of Pharmacology, University of California, San Diego, 9500 Gilman Drive, La Jolla, California 92093

Received June 18, 2004; E-mail: hckolb@scripps.edu

Abstract: The in situ click chemistry approach to lead discovery employs the biological target itself for assembling inhibitors from complementary building block reagents via irreversible connection chemistry. The present publication discusses the optimization of this target-guided strategy using acetylcholinesterase (AChE) as a test system. The application of liquid chromatography with mass spectroscopic detection in the selected ion mode for product identification greatly enhanced the sensitivity and reliability of this method. It enabled the testing of multicomponent mixtures, which may dramatically increase the in situ screening throughput. In addition to the previously reported in situ product *syn-TZ2PA6*, we discovered three new inhibitors, *syn-TZ2PA5*, *syn-TA2PZ6*, and *syn-TA2PZ5*, derived from tacrine and phenylphenanthridinium azides and acetylenes, in the reactions with *Electrophorus electricus* and mouse AChE. All in situ-generated compounds were extremely potent AChE inhibitors, because of the presence of multiple sites of interaction, which include the newly formed triazole nexus as a significant pharmacophore.

Introduction

The past decade has seen a paradigm shift in drug discovery from testing small numbers of “handcrafted” compounds and natural products to high-throughput screening of large combinatorial libraries.¹ These developments have gone hand in hand with dramatic improvements in methods for producing, handling, and screening large numbers of compounds.^{2–5} Despite these achievements, challenges related to the synthesis, purification, and diversity of compound libraries and the pharmacological properties of their members still exist,^{6,7} and combinatorial chemistry has not yet achieved its full potential.^{8,9} Since typically more than 99% of all compounds in a library are inactive in a given screen, methods for producing just the active compounds are highly desirable. Target-guided synthesis (TGS) seeks to address this challenge by using the target enzyme for assembling its own inhibitors from a collection of building block reagents.

Only building blocks that adhere to the protein’s binding sites react with each other to form highly potent inhibitors that simultaneously access multiple binding pockets within the protein. These target-guided approaches avoid the classical screening of large compound libraries altogether, and hit identification can be as simple as determining whether a given combination of building blocks has resulted in a product. Follow-up tests for determining the inhibitory potency, bioavailability, toxicity, and the development of structure–activity relationships (SAR) can then be limited to a small number of target-generated compounds, which may dramatically improve the efficiency of the discovery process.

The concept of target-guided synthesis was pioneered almost 20 years ago by Rideout et al., who observed a marked synergism between the cytotoxic effects of decanal and *N*-amino-guanidines, which was proposed to be due to the self-assembly of cytotoxic hydrazones inside cells.^{10,11} Since then, several approaches to target-guided synthesis have been explored: (1) dynamic combinatorial chemistry,^{12–21} (2) stepwise target-guided synthesis,^{22,23} and (3) kinetically controlled target-

[†] The Scripps Research Institute.

[‡] University of California, San Diego.

- (1) Nicolaou, K. C.; Hanks, R.; Hartwig, W. In *Handbook of Combinatorial Chemistry*; Nicolaou, K. C., Hanks, R., Hartwig, W., Eds.; Wiley-VCH: Weinheim, Germany, 2002; Vol. 1, pp 3–9.
- (2) Kolb, H. C.; Sharpless, K. B. *Drug Discovery Today* **2003**, *8*, 1128–1137.
- (3) Terrett, N. *Combinatorial Chemistry*; Oxford University Press: Oxford, U.K., 1998.
- (4) Nicolaou, K. C.; Hanks, R.; Hartwig, W. *Handbook of Combinatorial Chemistry*; Wiley-VCH: Weinheim, Germany, 2002; Vol. 1.
- (5) Nicolaou, K. C.; Hanks, R.; Hartwig, W. *Handbook of Combinatorial Chemistry*; Wiley-VCH: Weinheim, Germany, 2002; Vol. 2.
- (6) Kassel, D. B.; Myers, P. L. *Pharm. News* **2002**, *9*, 171–177.
- (7) Geysen, H. M.; Schoenen, F.; Wagner, D.; Wagner, R. *Nat. Rev. Drug Discovery* **2003**, *2*, 222–230.
- (8) Fixing the drugs pipeline. *The Economist*, March 11, 2004; available online at http://www.economist.com/printedition/displayStory.cfm?Story_ID=2477075.
- (9) Kubinyi, H. *Nat. Rev. Drug Discovery* **2003**, *2*, 665–668.

(10) Rideout, D. *Science* **1986**, *233*, 561–563.

(11) Rideout, D.; Calogeropoulou, T.; Jaworski, J.; McCarthy, M. *Biopolymers* **1990**, *29*, 247–262.

(12) Huc, I.; Lehn, J.-M. *Proc. Natl. Acad. Sci. U.S.A.* **1997**, *94*, 2106–2110.

(13) Ramstrom, O.; Lehn, J.-M. *ChemBioChem* **2000**, *1*, 41–48.

(14) Lehn, J.-M.; Eliseev, A. V. *Science* **2001**, *291*, 2331–2332.

(15) Bunyapaiboonsri, T.; Ramstrom, O.; Lohmann, S.; Lehn, J.-M.; Peng, L.; Goeldner, M. *ChemBioChem* **2001**, *2*, 438–444.

(16) Eliseev, A. V. *Pharm. News* **2002**, *9*, 207–215.

(17) Ramstrom, O.; Lehn, J.-M. *Nat. Rev. Drug Discovery* **2002**, *1*, 26–36.

(18) Otto, S. *Curr. Opin. Drug Discovery Dev.* **2003**, *6*, 509–520.

(19) Erlanson, D. A.; Braisted, A. C.; Raphael, D. R.; Randal, M.; Stroud, R. M.; Gordon, E. M.; Wells, J. A. *Proc. Natl. Acad. Sci. U.S.A.* **2000**, *97*, 9367–9372.

guided synthesis.^{24–31} The dynamic combinatorial chemistry approach introduced by Lehn et al.¹² relies on building blocks bearing complementary functional groups that react reversibly with each other to form a thermodynamically controlled mixture of products. In the presence of the enzyme, the equilibrium is skewed toward the compounds that show the highest affinity toward the enzyme. Their identification requires the equilibrium to be “frozen” (e.g., by hydride reduction or by lowering the pH) before analysis by HPLC or MS can be performed. The multistep variant of TGS makes only indirect use of the enzyme for inhibitor synthesis.^{22,23} In the first step, a library of building blocks is screened to identify candidates that bind to the enzyme. In the second step, the building blocks with the highest affinity are linked together using conventional combinatorial chemistry approaches. The library of “divalent” molecules is then screened for high affinity inhibitors using traditional assays. The kinetically controlled approach uses the enzyme target itself for the synthesis of inhibitors by equilibrium controlled sampling of various possible pairs of reactants until an irreversible reaction induced by the enzyme essentially connects the pair that best fits its binding pockets.^{24–31}

Recently, several successful applications of the kinetically controlled approach to TGS have been reported. For example, Benkovic and Boger have developed multisubstrate adduct inhibitors (MAI) of the enzyme glycinamide ribonucleotide transformylase (GAR Tfase) by enzyme-templated alkylation of one of its substrates with a folate-derived electrophile.^{26–28} More recently, Huc described a similar approach, in which inhibitors of carbonic anhydrase were generated by alkylation of a thiol with α -chloroketones in the presence of the Zn(II) enzyme.²⁹ Competition experiments revealed that the enzyme-templated reaction had produced mainly the alkylation product with the highest affinity for the target. Nicolaou and co-workers have utilized a target-accelerated combinatorial synthesis approach to develop dimeric derivatives of vancomycin.^{30,31} Appropriately functionalized monomeric vancomycin derivatives were subjected to olefin metathesis or disulfide formation in the presence of vancomycin's target, Ac-D-Ala-D-Ala or Ac₂-L-Lys-D-Ala-D-Ala, resulting in the formation of highly potent dimers.

The scope of most TGS methods is limited because of their use of highly reactive reagents (strong electrophiles or nucleo-

philes, metathesis catalysts etc.), which can react in many “unproductive” pathways, including ones that destroy the enzyme target. In contrast, the recently developed in situ click chemistry approach to kinetically controlled TGS²⁴ uses bio-orthogonal reactions and reagents, for example, the [1,3]-dipolar cycloaddition reaction³² between azides and acetylenes. This system is especially well-suited for TGS, since (a) the reaction is extremely slow at room temperature, despite the very high driving force that makes it irreversible, (b) it does not involve components that might disturb the binding sites (external reagents, catalysts, byproducts), and (c) the reactants are inert to biological molecules. Mock et al. had previously provided proof-of-concept by demonstrating that the azide/acetylene [1,3]-dipolar cycloaddition is accelerated by 4 to 5 orders of magnitude by the synthetic receptor cucurbituril to give exclusively the *anti*-triazole regioisomer.^{33–35}

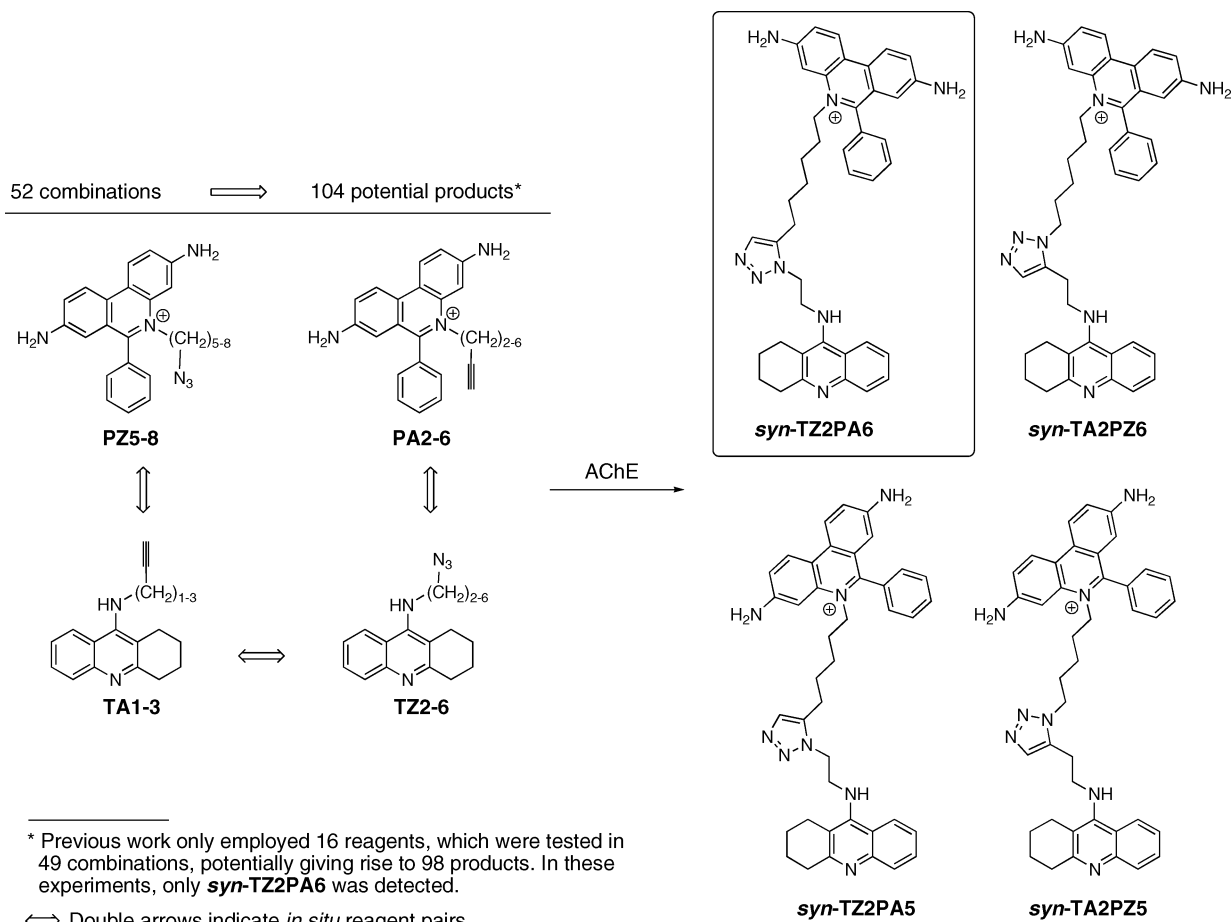
The biological target for the initial in situ click chemistry study, acetylcholinesterase (AChE), catalyzes the hydrolysis of the neurotransmitter acetylcholine and thus plays a key role in the central and peripheral nervous system.³⁶ Its inhibitors have been employed for over a century in various therapeutic regimens and to investigate the role of acetylcholine in neurotransmission.^{37,38} The catalytic site of the enzyme is located at the bottom of a 20 Å deep narrow gorge. A second, peripheral binding site is positioned at the other end of this gorge, near the protein surface.^{39,40} A building block library of azides and acetylenes based on the known site-specific inhibitors tacrine (active site ligand) and phenylphenanthridinium (peripheral site ligand) was developed to probe whether the enzyme would combine selected pairs of complementary reagents to synthesize its “divalent” inhibitors (cf. Scheme 1).²⁴

A series of 49 binary mixtures of these reagents was incubated with *Electrophorus electricus* AChE (electric eel AChE) at room temperature for 6 days, potentially giving rise to 98 products. Analysis of the crude reaction mixtures by desorption/ionization on silicon mass spectrometry⁴¹ (DIOS-MS) revealed only one product, **TZ2PA6**, which was shown by HPLC to be only the 1,5-disubstituted triazole (“*syn*-triazole”) (Scheme 1). This compound, formed by the enzyme, turned out to be the most potent noncovalent AChE inhibitor known to date, with K_d values between 77 fM (*Torpedo californica*) and 410 fM (murine AChE). In contrast, the *anti*-**TZ2PA6** isomer, not formed by the enzyme, is less active by 2 orders of magnitude.

Recent X-ray structures of both the *syn*- and *anti*-**TZ2PA6** mouse AChE complexes confirmed the multivalent nature of the protein ligand interactions, with the tacrine moiety accessing the active center of the enzyme and the phenylphenanthridinium group the peripheral site (Figure 1).²⁵ Interestingly, these studies

- (20) Erlanson, D. A.; Lam, J. W.; Wiesmann, C.; Luong, T. N.; Simmons, R. L.; DeLano, W. L.; Choong, I. C.; Burdett, M. T.; Flanagan, W. M.; Lee, D.; Gordon, E. M.; O'Brien, T. *Nat. Biotechnol.* **2003**, *21*, 308–314.
- (21) Ramström, O.; Lohmann, S.; Bunyapiboonsri, T.; Lehn, J.-M. *Chem. – Eur. J.* **2004**, *10*, 1711–1715.
- (22) Maly, D. J.; Choong, I. C.; Ellman, J. A. *Proc. Natl. Acad. Sci. U.S.A.* **2000**, *97*, 2419–2424.
- (23) Kehoe, J. W.; Maly, D. J.; Verdugo, D. E.; Armstrong, J. I.; Cook, B. N.; Ouyang, Y.-B.; Moore, K. L.; Ellman, J. A.; Bertozzi, C. R. *Bioorg. Med. Chem. Lett.* **2002**, *12*, 329–332.
- (24) Lewis, W. G.; Green, L. G.; Grynszpan, F.; Radic, Z.; Carlier, P. R.; Taylor, P.; Finn, M. G.; Sharpless, K. B. *Angew. Chem., Int. Ed.* **2002**, *41*, 1053–1057.
- (25) Bourne, Y.; Kolb, H. C.; Radic, Z.; Sharpless, K. B.; Taylor, P.; Marchot, P. *Proc. Natl. Acad. Sci. U.S.A.* **2004**, *101*, 1449–1454.
- (26) Inglesse, J.; Benkovic, S. J. *Tetrahedron* **1991**, *47*, 2351–2364.
- (27) Boger, D. L.; Haynes, N.-E.; Kitos, P. A.; Warren, M. S.; Ramcharan, J.; Marolewski, A. E.; Benkovic, S. J. *Bioorgan. Med. Chem.* **1997**, *5*, 1817–1830.
- (28) Greasley, S. E.; Marsilje, T. H.; Cai, H.; Baker, S.; Benkovic, S. J.; Boger, D. L.; Wilson, I. A. *Biochemistry* **2001**, *40*, 13538–13547.
- (29) Nguyen, R.; Huc, I. *Angew. Chem., Int. Ed.* **2001**, *40*, 1774–1776.
- (30) Nicolaou, K. C.; Hughes, R.; Cho, S. Y.; Winssinger, N.; Smethurst, C.; Labischinski, H.; Endermann, R. *Angew. Chem., Int. Ed.* **2000**, *39*, 3823–3828.
- (31) Nicolaou, K. C.; Hughes, R.; Cho, S. Y.; Winssinger, N.; Labischinski, H.; Endermann, R. *Chem. – Eur. J.* **2001**, *7*, 3824–3843.

- (32) Huisgen, R. In *1,3-Dipolar Cycloaddition Chemistry*; Padwa, A., Ed.; Wiley: New York, 1984; Vol. 1, pp 1–176.
- (33) Mock, W. L.; Irra, T. A.; Wepsiec, J. P.; Manimaran, T. L. *J. Org. Chem.* **1983**, *48*, 3619–3620.
- (34) Mock, W. L.; Irra, T. A.; Wepsiec, J. P.; Adhya, M. *J. Org. Chem.* **1989**, *54*, 5302–5308.
- (35) Mock, W. L. *Top. Curr. Chem.* **1995**, *175*, 1–24.
- (36) Taylor, P.; Radic, Z. *Annu. Rev. Pharmacol. Toxicol.* **1994**, *34*, 281–320.
- (37) Argyl-Robertson, D. *Edinburgh Med. J.* **1863**, *8*, 815–820.
- (38) Dale, H. H. *J. Pharmacol. Exp. Ther.* **1914**, *6*, 147–190.
- (39) Sussman, J. L.; Harel, M.; Frolow, F.; Oefner, C.; Goldman, A.; Tokar, L.; Silman, I. *Science* **1991**, *253*, 872–879.
- (40) Harel, M.; Schalk, I.; Ehret-Sabatier, L.; Bouet, F.; Goeldner, M.; Hirth, C.; Axelsen, P. H.; Silman, I.; Sussman, J. L. *Proc. Natl. Acad. Sci. U.S.A.* **1993**, *90*, 9031–9035.
- (41) Wei, J.; Buriak, J. M.; Siuzdak, G. *Nature* **1999**, *399*, 243–246.

Scheme 1. In Situ Click Chemistry Screening^a

^a Fifty-two binary mixtures of azide and alkyne building blocks were incubated with eel AChE, as indicated by the double arrows, potentially giving rise to 104 products. Previous work was done without **PZ5**, potentially giving rise to 98 products from 49 reagent combinations, and providing **syn-TZ2PA6** as the sole product of the *in situ* reaction with the enzyme.²⁴

revealed that the triazole unit, created by the azide/alkyne cycloaddition, engages in hydrogen bonding and stacking interactions with amino acid residues in the wall of the gorge. Several important conclusions can be drawn from this observation. First, triazoles are not just passive linkers, but rather active pharmacophores that may contribute significantly to protein binding, as in the case of the *in situ*-generated product, **syn-TZ2PA6**. Second, the tremendous rate acceleration by AChE⁴² is due not only to entropic effects, but also to an enthalpic stabilization of the triazole-like transition state, leading to the observed product. In a more general sense, it appears likely that an “*in situ* hit” is a good binder, because the same entropic and enthalpic factors that cause the observed rate acceleration may also stabilize the newly formed triazole in the complex and thus add to the overall binding interactions, which also involve the two residues that are held together by the triazole linker.

The higher potency of **syn-TZ2PA6** compared to the anti-isomer manifests itself in a strikingly different binding mode at the peripheral site. The phenylphenanthridinium moiety of the tightly bound *syn*-product inserts itself between tryptophan-286 and tyrosine-72 residues near the gorge rim (Figure 1),

causing the enzyme to adopt a minor abundance conformation in which the tryptophan residue swings out into the solvent to make room for the ligand. This conformation has never been seen before in AChE X-ray structures of the free enzyme or its inhibitor complexes. Thus, the *in situ* click chemistry approach allows one to identify conformations that associate with high affinity inhibitors and that would not be detected by conventional structural methods. These findings have interesting implications for drug discovery, as it is possible to trap a flexible enzyme in a minor abundance conformation by an inhibitor, which is formed inside its binding pockets through the irreversible reaction of complementary building blocks.

The goal of this study was to optimize the *in situ* approach to drug discovery and to investigate its scope. We started by optimizing the mass spectroscopy-based analysis method, since a highly sensitive and reliable method was deemed crucial for success. We then revisited the AChE system to search for additional *in situ* hits from binary azide/acetylene mixtures and from multireagent mixtures (combinatorial screening), to study the species dependence of product formation, and to determine *syn*/anti ratios and binding affinities for all products.

Results and Discussion

Optimization of the Analysis Method. Poor and variable levels of purity of the acetylcholinesterase enzyme make great demands on the analytical techniques used to detect the

(42) The enzyme-free reaction under these conditions ($[\text{TZ2}] = 4.6 \mu\text{M}$; $[\text{PA6}] = 24 \mu\text{M}$) is extremely slow, taking several thousand years to reach 50% conversion at 18 °C (second-order rate constant at 18 °C in 1-BuOH, $K = 1.9 \times 10^{-5} \text{ M}^{-1} \text{ min}^{-1}$ ²⁴). Apart from the expected entropic stabilization, the transition state may also experience stabilization through hydrogen bonding and stacking interactions with the protein.²⁵

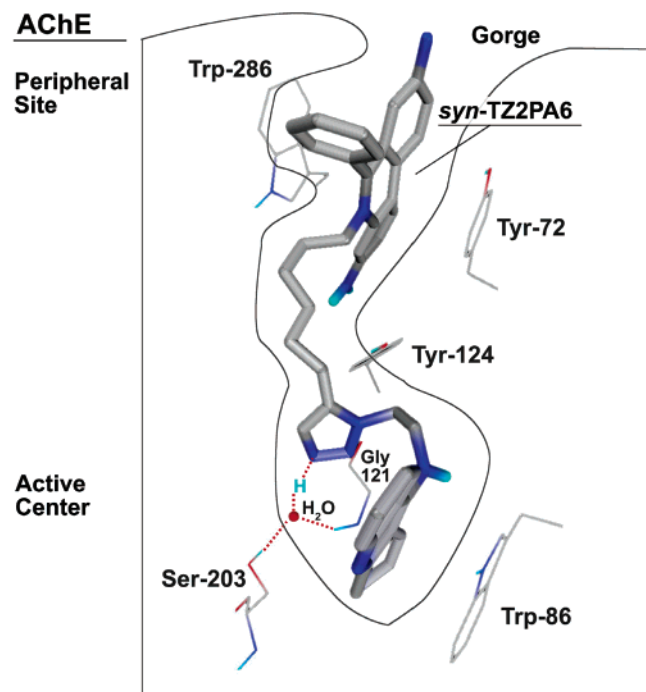


Figure 1. Schematic representation of the binding interactions between *syn*-TZ2PA6 and mouse AChE.²⁵

formation of templated inhibitors, especially when they are tightly bound. In previous experiments, the DIOS-MS method was found to be capable of detecting small quantities of new molecules in the presence of large amounts of protein, but signal-to-noise ratios were still very low. This issue has now been resolved by purifying the samples before MS analysis using standard LC/MS techniques with selected ion monitoring to increase sensitivity even further. *The analysis is extremely easy to perform, allowing crude reaction mixtures to be screened and products to be unambiguously identified by their molecular weights and retention times.*

The new analytical method was validated on the known *in situ* hit TZ2PA6. After incubating the building blocks TZ2 and PA6 with eel AChE for 6 h, analysis by LC/MS–SIM gave a distinct product signal with a characteristic molecular weight and retention time (Figure 2). Thus, the high sensitivity of this analysis method allowed us to reduce the incubation time from 6 days to as little as 6 h, thereby significantly enhancing the efficiency of lead discovery by *in situ* click chemistry.⁴³ Control experiments, in which mixtures of the same building blocks were incubated in the presence of bovine serum albumin (BSA) instead of AChE, or in the absence of any protein, failed to give detectable amounts of triazole.

In Situ Lead Discovery. Encouraged by these results, we decided to revisit the AChE system using a library of tacrine and phenylphenanthridinium building blocks (“T-P library”), which contained one additional member, PZ5, compared to previous work, and to screen for additional *in situ* hits with the

(43) The *in situ* screening experiments were generally performed with the following concentrations: 1 μM for the enzyme, 4.6 μM for tacrine components, and 24 μM for phenylphenanthridinium components. Because of the sensitive nature of the analysis method, the building block concentrations can be reduced to as low as 1 μM for tacrine reagents and 6 μM for phenylphenanthridinium reagents, without a significant loss of intensity of the product peak. However, lowering the phenylphenanthridinium component concentration to 1 μM dramatically decreased the reaction rate and makes the intensity of the product signal prohibitively small.

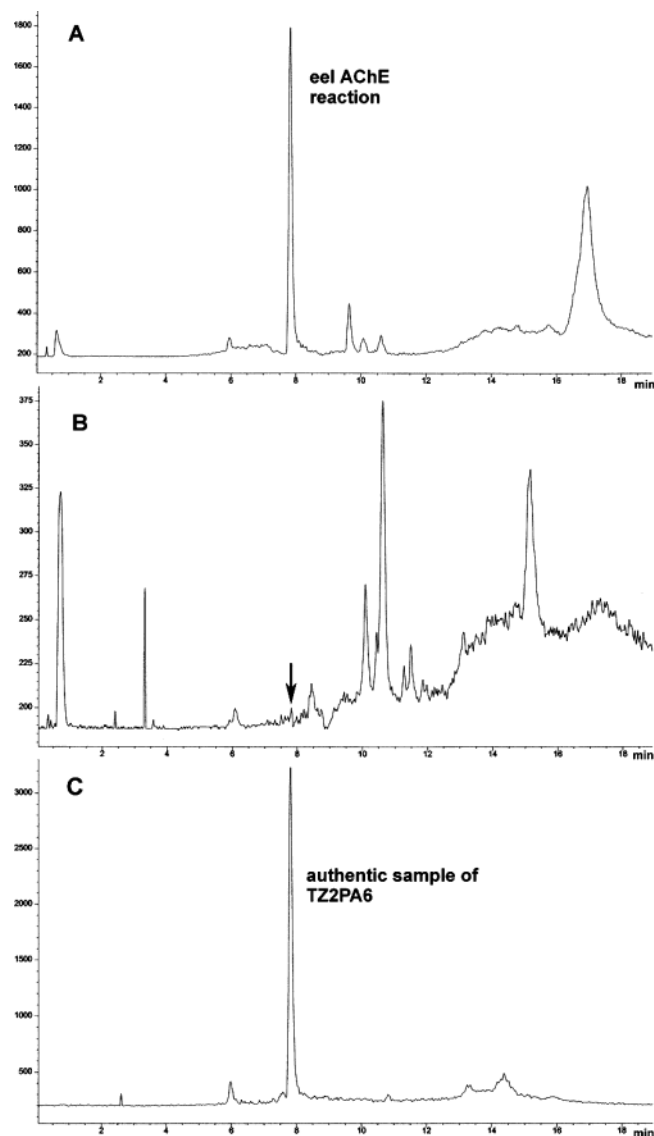


Figure 2. *In situ* hit identification by LC/MS–SIM, exemplified by the TZ2/PA6 pair. (A) TZ2 (4.6 μM) and PA6 (24 μM) after incubation with eel AChE (1.04 μM) at pH 7.5 for 6 h. (B) TZ2 and PA6 incubated in the presence of BSA (3 mg/mL) instead of AChE. The same trace is obtained in the absence of any protein (note that the Y-scale of the BSA trace is expanded 8.5 times compared to the eel AChE trace to clearly demonstrate the absence of any product in this sample). (C) Authentic sample of TZ2PA6.

more sensitive LC/MS–SIM method. In the “*in situ* screening mode”, potential hits are identified by looking for significant differences between the chromatograms of the enzyme reactions and the control reactions (BSA in place of AChE, absence of any protein). The potential hits are then validated by additional control experiments (e.g., performing the enzyme reaction in the presence of a known active site inhibitor) and eventually by comparing retention times with synthetic samples (cf. Table 3). This screening procedure led to the identification of three new hit compounds—TZ2PA5, TA2PZ6, and TA2PZ5—in addition to the known hit, TZ2PA6, by incubating 52 binary tacrine- and phenanthridinium-based azide/acetylene mixtures as illustrated in Scheme 1 (i.e., PZ5–8/TA1–3, PA2–6/TZ2–6, and TA1–3/TZ2–6) with eel AChE for 1 day. All hits were validated as described and by MALDI mass spectroscopy, which revealed distinct molecular ions for the respective products in

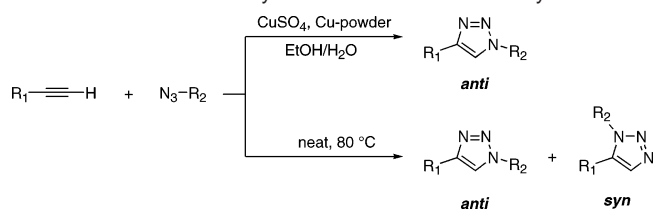
all four in situ reaction mixtures. Thus, only **TZ/PA** and **TA/PZ** combinations, not **TZ/TA** combinations, provided in situ hits.

Interestingly, all four hit compounds have the newly formed triazole moieties separated by two methylene units from the tacrine core. Other compounds with the same overall spacing between tacrine and phenanthridinium moieties, but a different location of the triazole (e.g., **TZ6PA2**), are not formed, suggesting that the triazole-genesis event is critically linked to a specific location in the protein's gorge. This notion is supported by the X-ray crystal structures of **TZ2PA6**/mouse AChE complexes,²⁵ which reveal that the triazole units are tightly bound inside the gorge through hydrogen bonding and stacking interactions (Figure 1). It is reasonable to assume that these product-stabilizing interactions in that location also favor the transition state leading to the product. Such active participation by the protein, in addition to entropic factors, would explain the dramatic rate acceleration observed in this system, over that for the uncatalyzed cycloaddition reaction.⁴²

Species Dependence. We decided to investigate the species dependence of product formation, since the X-ray studies were performed with mouse AChE, while eel enzyme was used for the in situ screen (58% sequence identity and 70% residue homology by NCBI Blast2).^{44,45} Incubation of binary azide/acetylene mixtures from the **T-P** building block library with mouse AChE and analysis by LC/MS–SIM provided the same four hit compounds—**TZ2PA6**, **TZ2PA5**, **TA2PZ6**, and **TA2PZ5**—as before. Thus, not only is mouse AChE able to make its inhibitors, it does so with the same building block preferences as the eel enzyme.

Combinatorial in Situ Screening. In situ click chemistry promises a big boost for lead discovery above all because it eliminates the need for high-throughput screening of large compound libraries, since the biological target itself has been forced to generate its inhibitors, which can readily be identified. Moreover, while previous experiments had used only binary azide/acetylene mixtures,²⁴ we have now found that the enzyme is able to select and assemble the best inhibitors from more complex mixtures of azide and acetylene building blocks. This not only reduces the amount of enzyme per reagent combination, but also increases the screening throughput. Multicomponent in situ click chemistry screening was made possible by the new LC/MS–SIM method, because of its higher sensitivity and greater reliability of product identification through chromatographic separation of the reaction components. In a proof-of-concept experiment, the azide **TZ2** and a mixture of four phenylphenanthridinium building blocks, **PA2-PA5**, were incubated with eel AChE under standard conditions at 37 °C overnight. LC/MS–SIM analysis of the reaction mixture showed the expected compound **TZ2PA5** to be the sole product. Encouraged by this success, we expanded this multicomponent approach to the entire tacrine azide/phenylphenanthridinium acetylene library. To avoid combinations with degenerate molecular weights (e.g., **TZ3PA5** has the same molecular weight as **TZ2PA6**), which would complicate product identification,

Scheme 2. Synthesis of Triazoles as Reference Compounds for the Determination of the *syn*/*anti* Ratio of in Situ Hits by HPLC^a



^a Equimolar *syn*- and *anti*-triazole mixtures were prepared by heating neat mixtures of the corresponding azides and alkynes at 80 °C for 6 days. The pure *anti*-regioisomers were readily prepared by the copper(I)-catalyzed reaction between the azide and alkyne reagents.^{46,47}

especially in view of the similar chromatographic behavior of the **TZ-PA** compounds, we decided to conduct the experiment in five batches: Mixtures of all five phenanthridinium acetylenes, **PA2-PA6**, were incubated with one tacrine azide at a time in the presence of mouse or eel AChE. Analysis by LC/MS–SIM revealed the expected hits, **TZ2PA5** and **TZ2PA6** (cf. Supporting Information). These experiments demonstrate that multicomponent screening is feasible, albeit at the cost of a slightly reduced sensitivity.

Determination of the *syn*/*anti* Selectivity. The X-ray cocrystal structures revealed that the more weakly bound *anti*-**TZ2PA6** has little effect on the enzyme conformation, whereas the higher affinity *syn*-**TZ2PA6** isomer, with its shorter spacer length between the tacrine and phenanthridinium moieties (the distance between the aromatic ring atoms of the tacrine and phenanthridinium moieties that are connected to the linker is 1.52 Å shorter in the *syn*-isomer, which is equivalent to about one C–C bond), forces the enzyme into a very different, and unprecedented conformation. This prompted the question of whether AChE would compensate for the deletion of one methylene unit in **TZ2PA5** by forming the “longer” *anti*-triazole instead of the “shorter” *syn*-isomer. Hence, we set out to study the *syn*/*anti* selectivity for the formation of **TZ2PA5** and the other new in situ hits by LC/MS–SIM. These efforts greatly benefited from the recently discovered Cu(I)-catalyzed process, which provides pure *anti*-triazoles from azides and terminal alkynes.^{46,47} Thus, **TZ2PA5**, **TA2PZ6**, and **TA2PZ5** were synthesized each as a mixture of *syn*- and *anti*-triazoles by the thermal cycloaddition reaction and as isomerically pure *anti*-triazoles by Cu(I) catalysis (Scheme 2).

Regioisomer assignment for the triazoles generated by AChE was accomplished by comparing the HPLC traces from the in situ reactions with authentic samples from the thermal and Cu(I)-catalyzed reactions (cf. Table 3).^{46,47} The new LC/MS–SIM system allowed us to obtain reliable results with single injections using only one-third of the amount of enzyme, compared to the previously used and much less sensitive HPLC–UV method. We were able to confirm the original assignment of the *syn*-geometry for enzyme-generated **TZ2PA6**,²⁴ and we found all the other products, **TZ2PA5**, **TA2PZ6**, and **TA2PZ5**, from both the eel and mouse AChE reactions to also contain almost exclusively *syn*-triazoles. Figure 3 exemplifies the results for the **TA2/PZ6** pair. While this is not surprising in the case of **TA2PZ6** in view of its similarity to **TZ2PA6**, we had expected

(44) The computation was performed at the Swiss Institute of Bioinformatics (SIB) using the BLAST network service. The SIB BLAST network service uses a server developed at SIB and the National Center for Biotechnology Information (NCBI) BLAST 2 software.

(45) Altschul, S. F.; Madden, T. L.; Schäffer, A. A.; Zhang, J.; Zhang, Z.; Miller, W.; Lipman, D. J. *Nucleic Acids Res.* **1997**, *25*, 3389–3402.

(46) Rostovtsev, V. V.; Green, L. G.; Fokin, V. V.; Sharpless, K. B. *Angew. Chem., Int. Ed.* **2002**, *41*, 2596–2599.

(47) Tornøe, C. W.; Christensen, C.; Meldal, M. *J. Org. Chem.* **2002**, *67*, 3057–3064.

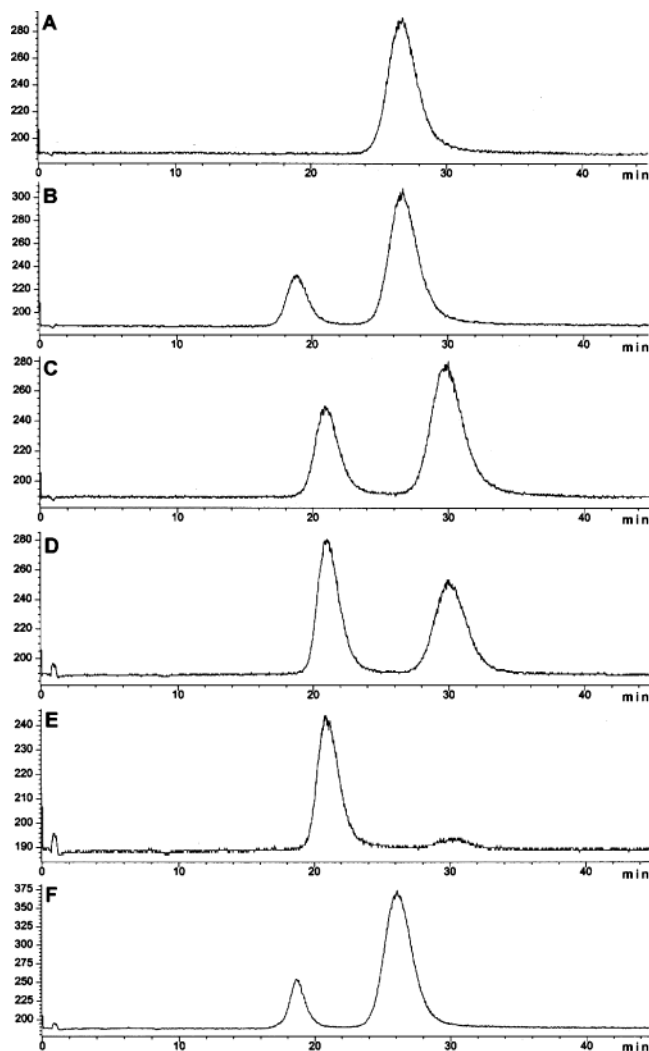


Figure 3. Regioisomer determination for mouse AChE-derived in situ hits. The in situ product, **TA2PZ6**, was compared by LC/MS–SIM to authentic samples from the thermal and the Cu(I)-catalyzed reactions.⁴⁸ (A) *anti*-**TA2PZ6** prepared by the Cu(I)-catalyzed reaction. (B) Co-injection of *anti*-**TA2PZ6** prepared by the Cu(I) catalysis and a mixture of *syn*- and *anti*-**TA2PZ6** prepared by the thermal reaction. (C) Mixture of *syn*- and *anti*-**TA2PZ6** prepared by the thermal reaction. (D) Co-injection of **TA2PZ6** prepared by the in situ click reaction and a mixture of *syn*- and *anti*-**TA2PZ6** prepared by the thermal reaction. (E) In situ click chemistry reaction. (F) Co-injection of the in situ click chemistry reaction and *anti*-**TA2PZ6**, prepared by the Cu(I)-catalyzed reaction.

the shorter linker in **TZ2PA5** and **TA2PZ5** to cause a switch into the “anti-mode”, which would have extended the linker by approximately 1.5 Å. These results suggest that the stereoelectronic requirements for effective catalysis of the cycloaddition inside the enzyme gorge are very strict. We are in the process of investigating this further by X-ray crystallography.

Binding Measurements. The equilibrium dissociation constants for the *syn*- and *anti*- **TA2PZ6**, **TA2PZ5**, **TZ2PA5**, and **TZ2PA6**²⁴ isomers, calculated as the ratios of their first-order dissociation and second-order association rate constants, are listed in Table 1, along with the corresponding free energy of binding values. All eight compounds were respectable inhibitors of both mouse and eel AChE, with dissociation constants in the femtomolar and picomolar range. Even though the femtomolar potency of the original in situ-generated inhibitor, *syn*-**TZ2PA6**, remains unsurpassed for both enzymes, the new in

situ hits, *syn*-**TZ2PA5**, *syn*-**TA2PZ6**, and *syn*-**TA2PZ5** are close. K_d values span 3 orders of magnitude, which is mainly due to an 1800-fold variability of dissociation rate constants k_{off} in the case of the eel enzyme, and 90-fold variability in the case of mouse AChE. In contrast, the on-rates k_{on} vary only by a factor of 3.

The range in dissociation constants is largest for the eel enzyme, where the free binding energy changes by 4.3 kcal/mol (295 K) from the tightest binder, *syn*-**TZ2PA6** (99 fM), to the weakest compound, *anti*-**TA2PZ5** (140 000 fM). In the case of the mouse enzyme, the free energy difference between the best binder, *syn*-**TZ2PA6** (410 fM), and the weakest inhibitor, *anti*-**TA2PZ5** (44 000 fM), is only 2.7 kcal/mol. We were able to derive a linear free energy relationship from the binding data, which allows us to calculate binding energy changes upon modifying the ligand structure, for example, from *syn*-**TZ2PA6** to *anti*-**TA2PZ5**. The mean values for the energy increments for each structural modification are summarized in Table 2. Further details are provided in the Supporting Information.

The energy differences derived from the linear free energy relationship closely match the experimental values. For example, *syn*-**TZ2PA6** was calculated to be 4.3 kcal/mol more tightly bound than *anti*-**TA2PZ5** in the eel AChE case (3.1 kcal/mol for *syn*-to-*anti* isomerization, plus 0.15 kcal/mol for linker shortening, plus 1.0 kcal/mol for inversion of triazole orientation), whereas the difference is only 3.0 kcal/mol in the mouse enzyme case (1.9 kcal/mol for *syn*-to-*anti* isomerization, plus 0.7 kcal/mol for linker shortening, plus 0.4 kcal/mol for inversion of triazole orientation). The fact that a linear free energy relationship can be successfully applied suggests that the inhibitors are stabilized by largely independent multipoint interactions with the protein, and the data indicate that not only the tacrine and phenanthridinium moieties but also the triazole ring are involved in binding. Consequently, the triazole apparently functions as an independent pharmacophore.

Many of the structure–activity trends revealed in Table 1 are species-dependent. In general, eel AChE rate constants are more dependent on the triazole substitution pattern, while mouse AChE is more sensitive to changes in linker length. For example, the *syn*/*anti* preference is much greater for eel AChE (average preference: 3.1 kcal/mol \pm 0.3 kcal/mol, 200-fold) than for mouse AChE (average preference: 1.9 kcal/mol \pm 0.4 kcal/mol, 26-fold). Also, the inversion of triazole ring orientation (**TZ2PA6** \rightarrow **TA2PZ6**, **TZ2PA5** \rightarrow **TA2PZ5**) leads to a marked increase of the dissociation rate in the case of the eel enzyme (1.0 \pm 0.2 kcal/mol, 5.5-fold), while the effects for the mouse enzyme were less pronounced (0.4 \pm 0.4 kcal/mol, 2-fold). For the *syn*-triazole inhibitors, which are the products of the in situ click reactions, the shortening of the linker between the triazole and phenanthridinium moieties from six (*syn*-**TZ2PA6**, *syn*-**TA2PZ6**) to five methylene groups (*syn*-**TZ2PA5**, *syn*-**TA2PZ5**) has only a very small effect on the dissociation constants K_d for the eel enzyme (−0.12 kcal/mol, 0.8-fold), while it leads to a 5-fold increase in the case of mouse AChE (0.97 kcal/mol). In contrast, for the *anti*-triazoles, the shortening of the linker reduces the binding affinity for both the mouse and eel enzymes.

The observed species-specific differences of rate and binding trends indicate that the two enzymes interact differently with

Table 1. Interaction Constants and Free Energies of Binding ($-RT \ln K_d$ at $T = 295$ K) of Triazole Inhibitors with Acetylcholinesterases

inhibitor		k_{on} ($10^{10} \text{ M}^{-1} \text{ min}^{-1}$)	k_{off} (min^{-1})	K_d (fM)	$-RT \ln K_d$ (kcal mol $^{-1}$)	AChE source
TA2PZ5	<i>syn</i>	1.5	0.0081	540	16.6	<i>Electrophorus</i>
		1.5	0.045	3 000	15.6	mouse
	<i>anti</i>	0.98	1.4	140 000	13.3	<i>Electrophorus</i>
		1.1	0.50	44 000	14.0	mouse
TZ2PA5	<i>syn</i>	0.76	0.00077	100	17.5	<i>Electrophorus</i>
		1.2	0.028	2300	15.7	mouse
	<i>anti</i>	0.90	0.38	42 000	14.0	<i>Electrophorus</i>
		1.3	0.43	33 000	14.1	mouse
TA2PZ6	<i>syn</i>	1.2	0.010	830	16.3	<i>Electrophorus</i>
		1.4	0.0086	610	16.5	mouse
	<i>anti</i>	1.4	1.4	100 000	13.5	<i>Electrophorus</i>
		1.7	0.71	42 000	14.0	mouse
TZ2PA6	<i>syn</i>	1.5	0.0015	99	17.6	<i>Electrophorus</i>
		1.7	0.0071	410	16.7	mouse
	<i>anti</i>	1.8	0.25	14 000	14.7	<i>Electrophorus</i>
		2.5	0.22	8900	14.9	mouse

Table 2. Energy Increments for Structural Changes

structural change	mean $\Delta(-RT \ln K_d)$ (kcal mol $^{-1}$)	AChE source
<i>syn</i> \rightarrow <i>anti</i>	3.1 \pm 0.3	<i>Electrophorus</i>
	1.9 \pm 0.4	mouse
P6 \rightarrow P5	0.15 \pm 0.38	<i>Electrophorus</i>
	0.69 \pm 0.45	mouse
TZ \rightarrow TA	1.0 \pm 0.2	<i>Electrophorus</i>
	0.37 \pm 0.36	mouse
Σ (<i>syn</i> \rightarrow <i>anti</i> + P6 \rightarrow P5 + TZ \rightarrow TA)	$\Sigma \Delta(-RT \ln K_d)^a$ 4.3 (4.3)	<i>Electrophorus</i>
	3.0 (2.7)	mouse

^a Energy difference values calculated from increments are shown in bold typeface; experimental values are in parentheses.

Table 3. Analytical HPLC Conditions for Selected Compounds

compound	elution solvent mixture				retention time (min)
	A (%)	B (%)	C (%)	D (%)	
TZ2PA6^a	<i>syn</i>		56	44	28.4
	<i>anti</i>		56	44	34.6
TZ2PA5^a	<i>syn</i>		56	44	19.2
	<i>anti</i>		56	44	25.2
TA2PZ6^a	<i>syn</i>		54	46	20.8
	<i>anti</i>		54	46	29.9
TA2PZ5^a	<i>syn</i>		56	44	20.6
	<i>anti</i>		56	44	24.7
TZ2PA6^{b,c}	gradient	gradient			7.8
TZ2PA5^{b,c}	gradient	gradient			7.6
TA2PZ6^{b,c}	gradient	gradient			7.7
TA2PZ5^{b,c}	gradient	gradient			7.6
TA2^c	gradient	gradient			7.2
TZ2^c	gradient	gradient			7.3
PA5^c	gradient	gradient			8.6
PA6^c	gradient	gradient			8.4
PZ5^c	gradient	gradient			8.5
PZ6^c	gradient	gradient			8.7

^a Analytical HPLC column Cyclobond I 2000 DMP (10 \times 4.6 mm) preceded by a Phenomenex C18 ODS guard column. Isocratic elution at 0.5 mL \cdot min $^{-1}$. ^b Mixture of *syn*- and *anti*-triazoles. ^c Analytical column Zorbax SB-C8 (2.1 \times 50 mm) preceded by a Phenomenex C18 ODS guard column. Flow rate 0.3 mL \cdot min $^{-1}$. At 0 min, elution solvent mixture A/B = 100/0, at 10 min, elution solvent mixture A/B = 0/100, at 18 min, elution solvent mixture A/B = 0/100.

the products of the in situ reactions and their anti-congeners. While this may not be seen as surprising in view of the relatively low sequence identity (58%) between the two enzymes, detailed analysis of the primary structures reveals a fully conserved interior of the active center gorge starting from Trp286 of the

peripheral site and ending with Trp86 at the bottom of the gorge. Thus, more global properties of the gorge, such as its overall shape or flexibility, not directly and exclusively determined by conserved interior residues, may be responsible for the observed trends.

Experimental Section

General. Reactions requiring anhydrous conditions were run under nitrogen in glassware flame dried under vacuum. Reagents were purchased from Acros or Aldrich and were used as received. Reaction progress was monitored by TLC using Merck silica gel 60 F-254 with detection by UV. Silica gel 60 (Merck 40–63 μ m) was used for column chromatography. The preparation of the library of tacrine and phenylphenanthridinium building blocks was published in a previous article.²⁴

Instrumentation. ¹H NMR and ¹³C NMR spectra were recorded with Bruker DRX-600, Bruker DRX-500, or Varian Inova-400 spectrometers. Proton magnetic resonance (¹H NMR) spectra were recorded at 600, 500, or 400 MHz. Data are presented as follows: chemical shift (ppm), multiplicity (*s* = singlet, *d* = doublet, *t* = triplet, *q* = quartet, *quin* = quintet, *m* = multiplet), coupling constant (Hz), and integration. Carbon magnetic resonance (¹³C NMR) spectra were recorded at 150, 125, or 100 MHz. Data for ¹³C NMR are reported in terms of chemical shifts (ppm). Infrared spectra were recorded on an Avatar 370 Fourier transform spectrometer (IR) and are reported as follows: wavenumbers (cm $^{-1}$), description (*w* = weak, *m* = medium, *s* = strong, *b* = broad). High-resolution mass spectra (HRMS) were recorded at the mass spectrometry facility at The Scripps Research Institute, La Jolla, CA. HPLC was performed on an Agilent 1100 LC/MSD with an Agilent 1100 SL mass spectrometer, using four different elution solvents: elution solvent A (0.05% TFA in H₂O), elution solvent B (0.05% TFA in CH₃CN), elution solvent C (1% Me₃N/formic acid in H₂O, pH = 7.5), and elution solvent D (MeOH).

General Procedures for in Situ Click Chemistry Experiments. **Determination of Acetylcholinesterase Concentrations.** The concentrations of the eel and mouse enzymes were calculated in terms of molarity of active sites based on quantitative measurements of enzyme activity. Commercially available preparations of *Electrophorus* AChE were found to contain approximately 10% active enzyme. The concentration was determined by quantitative measurement of AChE activity using the Ellman assay as previously described.²⁴ Concentrations of highly purified preparations of mouse AChE, prepared from expression in HEK cells using a recombinant cDNA,^{49,50} containing

(48) All samples were analyzed by LC/MS–SIM with electrospray detection on a Cyclobond I 2000 DMP column (4.6 \times 100 mm, preceded by a Phenomenex C18 ODS guard column) using isocratic elution conditions.

practically homogeneous enzyme, were determined by quantitative measurement of AChE activity using the Ellman assay and comparing that activity to previously determined values⁴⁹ of k_{cat} in quantitative agreement with band intensities in gels of polyacrylamide gel electrophoresis.

In Situ Click Chemistry Screening Procedure for Binary Reagent Mixtures. The tacrine component (i.e., **TZ2** through **TZ6** or **TA1** through **TA3** dissolved in MeOH) was added to $\sim 1 \mu\text{M}$ solutions of *Electrophorus* AChE (type V-S, Sigma) or mouse AChE^{49,50} in buffer (2 mM ammonium citrate, 100 mM NaCl, pH = 7.3–7.5) followed immediately by one of the phenylphenanthridinium components (i.e., **PA2** through **PA6** and **PZ5** through **PZ8**, respectively) and mixed. The final concentrations were as follows: eel or mouse AChE: 1 μM ; tacrine component: 4.6 μM ; phenylphenanthridinium component: 24 μM ; MeOH: 1.5%. Under these conditions, approximately 99.5% of the active sites are in complex with the tacrine component ($K_{\text{d}}(\text{tacrine}) = 18 \text{ nM}$ for mAChE²⁴), and 95% of the peripheral binding sites are in complex with the phenanthridinium reagent ($K_{\text{d}}(\text{propidium}) = 1100 \text{ nM}$ ²⁴). Each reaction mixture was incubated at 37 °C for at least 6 h. Samples of the reactions were injected directly (15 μL) into the LC/MSD instrument to perform LC/MS–SIM analysis (Zorbax SB-C8 reverse-phase column, preceded by a Phenomenex C18 guard column, electrospray ionization and mass spectroscopic detection in the positive selected-ion mode, tuned to the expected molecular mass of the product). The cycloaddition products were identified by their retention times and molecular weights. Control experiments in the absence of enzyme or in the presence of BSA instead of enzyme failed to produce product signals. For the BSA experiments, AChE was substituted for bovine serum albumin (3 mg/mL). Methanol (1:1 dilution) was added to the reaction mixture prior to LC/MS–SIM analysis to prevent precipitation of the expected **TZ-PA** triazole product.

In Situ Click Chemistry Screening Procedure for Multicomponent Incubations. A methanolic solution (11.0 μL) of phenylphenanthridinium building blocks **PA2**–**PA6** (stock solution contains 400 μM of each building block) was added to a solution of mouse AChE (1.1 mL of 1 μM AChE, 2 mM ammonium citrate, 100 mM NaCl, pH = 7.3–7.5). This mixture was then distributed into five different Eppendorf vials (198 μL per vial), and each sample was mixed with one of the tacrine building blocks (**TZ2**–**TZ6**; 2.0 μL of a 1.92 mM methanolic stock solution). The final concentrations were as follows: mouse AChE: 1 μM ; tacrine component: 19.2 μM ; phenylphenanthridinium component: 4.0 μM ; MeOH: 2%. Each reaction mixture was incubated at 37 °C for at least 24 h. Samples of the reactions were injected directly (15 μL) into the LC/MSD instrument to perform LC/MS–SIM analysis. The cycloaddition products were identified by their retention times and molecular weights.

LC–MS Analysis. Although the analysis by DIOS-MS, as described previously,²⁴ required only submicroliter amounts for a single measurement, the results suffered from poor signal/noise ratios. In contrast, the LC/MS method with selected ion monitoring is considerably more sensitive, with detection limits in the nanomolar range. The eluent contains 0.05% TFA, which results in fast denaturation of the enzyme and release of product on the column (we have obtained a linear correlation between the concentration of *syn*-**TZ2PA6** and its LC/MS–SIM signal in the presence of an excess of mAChE, cf. Supporting Information, section 2). This allows the compound, e.g., **TZ2PA6**, to be readily detected in the presence of the enzyme at concentrations as low as 4 nM, which corresponds to 0.4% of the used enzyme active site concentration. The analyses were performed on an Agilent 1100 LC/MSD instrument by reverse-phase HPLC using a 30 \times 2.1 mm Zorbax SB-C8 column, preceded by a Phenomenex C18 ODS guard

column. The injection volume was 15–30 μL , and the components were eluted using a gradient (flow rate at 0.3 mL \cdot min⁻¹; at 0 min elution solvent mixture A/B = 100/0; at 10 min elution solvent mixture A/B = 0/100; at 18 min elution solvent mixture A/B = 0/100). The mass spectrometer was set to the positive ion mode with selected ion monitoring of only the expected m/z . Under these conditions, in situ click chemistry products derived from binary building block mixtures are readily detectable after 6 h of incubation in the presence of enzyme.

Regioisomer Determination. The sensitive LC/MS–SIM method was employed for determining the regioisomer distribution of the in situ click chemistry products **TZ2PA6**, **TZ2PA5**, **TA2PZ5**, and **TA2PZ6**. The assignment was accomplished by comparing the retention times of the in situ products with authentic samples, prepared by thermal cycloaddition (yielding an approximately 1:1 mixture of regioisomers) and copper-catalyzed azide/acetylene reaction (yielding pure anti-regioisomers). The in situ reaction mixtures were injected directly (15–80 μL) into the LC/MS as well as co-injected with the reference compounds. Comparison of all traces revealed that the *syn*-isomers were formed preferentially in situ. The chromatography was performed on a 100 \times 4.6 mm Cyclobond I 2000 DMP column, preceded by a Phenomenex C18 ODS guard column. The MS detector settings used were the same as those for the screening of reactions.

Synthesis of Building Blocks and Reference Compounds.

CAUTION! All of the compounds described here (and especially the most potent polyvalent inhibitors) are potentially neurotoxic. They must be handled with extreme care by trained personnel.

Tacrine Building Block TA2. A mixture of 9-chloro-1,2,3,4-tetrahydroacridine (1.0 g, 4.61 mmol), but-3-ynylammonium chloride (0.54 g, 5.05 mmol), and triethylamine (0.93 g, 9.2 mmol) in pentanol (3 mL) was heated at reflux for 16 h. The reaction mixture was diluted with CH₂Cl₂, washed with saturated NaHCO₃ solution, dried over MgSO₄, and concentrated. The residue was purified by chromatography (EtOAc/MeOH = 9/1) to give pure alkyne **TA2** (1.06 g, 4.23 mmol, 92%). ¹H NMR (400 MHz, CD₃OD): δ 8.44 (*d*, $J = 8.6 \text{ Hz}$, 1H), 8.04 (*d*, $J = 8.1 \text{ Hz}$, 1H), 7.95 (*t*, $J = 6.4 \text{ Hz}$, 1H), 7.84 (*t*, $J = 7.5 \text{ Hz}$, 1H), 7.56 (*t*, $J = 7.5 \text{ Hz}$, 1H), 3.92 (*m*, 2H), 3.04 (*m*, 2H), 2.76–2.60 (*m*, 4H), 2.51 (*t*, $J = 2.1 \text{ Hz}$, 1H), 1.81 (*m*, 4H) ppm; ¹³C NMR (400 MHz, CD₃OD): δ 156.8, 152.0, 138.6, 133.4, 126.1, 125.8, 120.0, 116.7, 112.5, 82.1, 74.1, 46.8, 28.8, 25.06, 22.3, 21.1, 20.6 ppm; UV–vis (H₂O/CH₃CN/TFA = 40/60/0.05): λ_{max} (relative intensities) 248 (100%), 346 (43%) nm; IR: ν 3340 (br), 3220 (s), 2940 (m), 2860 (m), 1620 (s), 1580 (w), 1560 (w), 1500 (m), 1470 (m), 1400 (w), 1350 (w), 1260 (m), 1120 (w), 1080 (w), 1030 (m), 950 (w), 830 (m) cm⁻¹; HRMS (ESI-TOF) calcd for C₁₇H₁₉N₂ (MH⁺), 251.1543; found, 251.1547.

Phenylphenanthridinium Building Blocks. Building blocks **PA5**, **PZ6**, and **PZ5** were prepared according to previously reported methods.²⁴

PA5: ¹H NMR (500 MHz, CD₃OD): δ 8.64 (*d*, $J = 9.1 \text{ Hz}$, 1H), 8.54 (*d*, $J = 9.2 \text{ Hz}$, 1H), 7.88–7.76 (*m*, 3H), 7.64–7.52 (*m*, 3H), 7.40–7.34 (*m*, 2H), 6.46 (*d*, $J = 2.2 \text{ Hz}$, 1H), 4.52 (*t*, $J = 7.9 \text{ Hz}$, 2H), 2.22 (*t*, $J = 2.5 \text{ Hz}$, 1H), 2.16–2.12 (*m*, 4H), 1.44–1.32 (*m*, 4H) ppm; ¹³C NMR (500 MHz, CD₃OD): δ 160.2, 153.1, 149.7, 136.5, 133.7, 132.3, 130.8, 130.1, 129.9, 129.6, 126.8, 126.0, 123.9, 121.5, 119.7, 110.4, 99.8, 84.5, 70.1, 54.9, 29.4, 28.7, 26.5, 18.2 ppm; UV–vis (H₂O/CH₃CN/TFA = 40/60/0.05): λ_{max} (relative intensities) 293 (100%), 324 (30%) nm; IR: ν 3360 (m), 3240 (m), 2960 (s), 2930 (s), 2870 (m), 1730 (s), 1620 (s), 1580 (w), 1490 (m), 1470 (m), 1260 (s), 1160 (m), 1080 (m), 1030 (s), 830 (w) cm⁻¹; HRMS (ESI-TOF) calcd for C₂₆H₂₆N₃ (M⁺), 380.2127; found, 321.2126.

PZ5: ¹H NMR (500 MHz, CD₃OD): δ 8.62 (*d*, $J = 9.1 \text{ Hz}$, 1H), 8.59 (*d*, $J = 9.2 \text{ Hz}$, 1H), 7.83–7.72 (*m*, 3H), 7.68–7.54 (*m*, 3H), 7.38–7.32 (*m*, 2H), 6.46 (*d*, $J = 2.4 \text{ Hz}$, 1H), 4.52 (*t*, $J = 8.1 \text{ Hz}$, 2H), 2.06–1.88 (*m*, 2H), 1.78–1.26 (*m*, 6H) ppm; ¹³C NMR (500 MHz, CD₃OD): δ 159.9, 152.7, 149.5, 136.4, 133.8, 132.3, 130.8, 130.1, 129.8, 129.4, 126.7, 126.1, 123.8, 121.2, 119.8, 110.4, 99.8, 52.1, 31.0,

(49) Radic, Z.; Pickering, N. A.; Vellom, D. C.; Camp, S.; Taylor, P. *Biochemistry* **1993**, *32*, 12074–12084.

(50) Marchot, P.; Ravelli, R. B. G.; Raves, M. L.; Bourne, Y.; Vellom, D. C.; Kanter, J.; Camp, S.; Sussman, J. L.; Taylor, P. *Protein Sci.* **1996**, *5*, 672–679.

29.4, 29.1, 24.8 ppm; UV-vis (H₂O/CH₃CN/TFA = 40/60/0.05): λ_{\max} (relative intensities) 292 (100%), 324 (30%) nm; IR: ν 3440 (w), 3360 (m), 3240 (m), 2930 (s), 2860 (s), 2090 (s), 1640 (s), 1630 (s), 1500 (m), 1470 (w), 1260 (s), 1160 (s), 1030 (s), 830 (w) cm⁻¹; HRMS (ESI-TOF) calcd for C₂₄H₂₅N₆ (M⁺), 397.2141; found, 397.2130.

PZ6: ¹H NMR (600 MHz, CD₃OD): δ 8.63 (*d*, *J* = 9.1 Hz, 1H), 8.56 (*d*, *J* = 9.2, 1H), 7.82–7.76 (*m*, 3H), 7.64–7.54 (*m*, 3H), 7.39–7.33 (*m*, 2H), 6.48 (*d*, *J* = 2.4, 1H), 3.46–3.29 (*m*, 2H), 2.06–1.88 (*m*, 2H), 1.80–1.62 (*m*, 4H), 1.22–1.58 (*m*, 4H) ppm; ¹³C NMR (600 MHz, CD₃OD): δ 160.3, 153.0, 149.7, 136.5, 133.8, 132.3, 130.9, 130.1, 129.9, 129.6, 126.8, 126.0, 123.8, 121.6, 119.7, 110.4, 99.8, 52.4, 30.9, 29.7, 27.5, 27.1, 26.9 ppm; UV-vis (H₂O/CH₃CN/TFA = 40/60/0.05): λ_{\max} (relative intensities) 292 (100%), 324 (28%) nm; IR: ν 3450 (w), 3360 (m), 3240 (m), 2930 (s), 2860 (m), 2100 (s), 1640 (m), 1630 (m), 1500 (m), 1460 (w), 1260 (s), 1160 (s), 1030 (s), 830 (w) cm⁻¹; HRMS (ESI-TOF) calcd for C₂₅H₂₇N₆ (M⁺), 411.2297; found, 411.2292.

General Procedure for the Preparation of Regioisomerically Pure *syn*-Triazoles. Azide (50 μ mol) and alkyne (50 μ mol) were dissolved in methanol (1 mL), and the solvent was subsequently removed under reduced pressure. The residue was heated in an oven at 80–120 °C for 4–7 days, affording the corresponding triazole as a *syn/anti* mixture of approximately 1:1. The regioisomers were separated by semipreparative HPLC (Cyclobond I 2000 DMP, 250 \times 10 mm) to yield regioisomerically pure triazoles.

***syn*-TZ2PA5:** ¹H NMR (600 MHz, CD₃OD): δ 8.62 (*d*, *J* = 9.1 Hz, 1H), 8.56 (*d*, *J* = 9.2 Hz, 1H), 8.24 (*d*, *J* = 8.2 Hz, 2H), 7.74–7.16 (*m*, 11 H), 6.45 (*d*, *J* = 2.0 Hz, 1H), 4.66 (*t*, *J* = 7.3 Hz, 2H), 4.37 (*m*, 2H), 4.18 (*t*, *J* = 7.2 Hz, 2H), 2.97 (*s*, 2H), 2.57 (*t*, *J* = 6.9 Hz, 2H), 1.93–1.76 (*m*, 6H), 1.41–1.12 (*m*, 6H) ppm; UV-vis (H₂O/CH₃CN/TFA = 40/60/0.05): λ_{\max} (relative intensities) 248 (98%), 292 (100%), 333 (52%) nm; IR: ν 3340 (br), 2950 (m), 2840 (m), 1640 (w), 1620 (w), 1580 (m), 1520 (w), 1500 (w), 1450 (w), 1410 (w), 1320 (w), 1260 (w), 1230 (w), 1110 (w), 1020 (s) cm⁻¹; HRMS (ESI-TOF) calcd for C₄₁H₄₃N₈ (M⁺), 647.3611; found, 647.3595.

***syn*-TA2PZ6:** ¹H NMR (500 MHz, CD₃OD): δ 8.62 (*d*, *J* = 9.1 Hz, 1H), 8.57 (*d*, *J* = 9.2 Hz, 1H), 8.24 (*d*, *J* = 8.2 Hz, 2H), 7.72–7.12 (*m*, 11 H), 6.41 (*d*, *J* = 2.2 Hz, 1H), 4.70–4.37 (*m*, 4H), 4.30–4.13 (*m*, 2H), 2.83 (*s*, 2H), 2.78–2.60 (*m*, 4H), 1.93–1.76 (*m*, 6H), 1.41–1.12 (*m*, 6H) ppm; UV-vis (H₂O/CH₃CN/TFA = 40/60/0.05): λ_{\max} (relative intensities) 248 (97%), 293 (100%), 334 (55%) nm; IR: ν 3310 (br), 2930 (m), 2860 (m), 1690 (w), 1620 (m), 1590 (m), 1520 (w), 1490 (w), 1450 (m), 1410 (w), 1340 (m), 1260 (m), 1180 (w), 1150 (w), 1050 (s), 950 (w), 830 (w) cm⁻¹; HRMS (ESI-TOF) calcd for C₄₂H₄₅N₈ (M⁺), 661.3767; found, 661.3753.

***syn*-TA2PZ5:** ¹H NMR (400 MHz, CD₃OD): δ 8.68–8.23 (*m*, 4H), 7.77–7.10 (*m*, 11 H), 6.45 (*d*, *J* = 2.3 Hz, 1H), 4.56–4.17 (*m*, 6H), 3.01 (*s*, 2H), 2.62 (*t*, *J* = 7.48 Hz, 2H), 1.93–1.79 (*m*, 6H), 1.38–1.15 (*m*, 6H) ppm; UV-vis (H₂O/CH₃CN/TFA = 40/60/0.05): λ_{\max} (relative intensities) 247 (97%), 293 (100%), 334 (53%) nm; IR: ν 3350 (br), 2940 (m), 2850 (w), 1620 (w), 1590 (m), 1520 (w), 1480 (w), 1460 (m), 1410 (m), 1350 (m), 1250 (m), 1180 (w), 1160 (w), 1080 (w), 1020 (s), 950 (w), 830 (w) cm⁻¹; HRMS (ESI-TOF) calcd for C₄₁H₄₃N₈ (M⁺), 647.3611; found, 647.3596.

General Procedure for the Synthesis of Isomerically Pure *anti*-Triazoles. An aqueous CuSO₄ solution (100 mM, 25 μ L) and copper powder (2 mg) were added to a solution of azide (50 μ mol) and alkyne (50 μ mol) in ethanol (200 μ L). The reaction mixture was stirred at room temperature for 2–4 days. The *anti*-triazole was purified by semipreparative HPLC.

***anti*-TZ2PA5:** ¹H NMR (600 MHz, CD₃OD): δ 8.62 (*d*, *J* = 9.1 Hz, 1H), 8.56 (*d*, *J* = 9.2 Hz, 1H), 7.96 (*d*, *J* = 8.6 Hz, 2H), 7.72–7.24 (*m*, 11 H), 6.38 (*d*, *J* = 2.3 Hz, 1H), 4.70 (*t*, *J* = 7.8 Hz, 2H), 4.37 (*m*, 2H), 4.21 (*t*, *J* = 6.1 Hz, 2H), 2.91 (*s*, 2H), 2.53 (*t*, *J* = 7.4 Hz, 2H), 1.88–1.72 (*m*, 6H), 1.41–1.16 (*m*, 6H) ppm; UV-vis (H₂O/CH₃CN/TFA = 40/60/0.05): λ_{\max} (relative intensities) 248 (96%), 292

(100%), 334 (51%) nm; IR: ν 3340 (br), 2930 (m), 2870 (w), 2100 (s), 1730 (w), 1700 (w), 1590 (s), 1520 (w), 1490 (w), 1450 (m), 1370 (m), 1350 (m), 1230 (m), 1180 (m), 1160 (m), 1040 (w), 950 (m), 840 (m) cm⁻¹; HRMS (ESI-TOF) calcd for C₄₁H₄₃N₈ (M⁺), 647.3611; found, 647.3597.

***anti*-TA2PZ6:** ¹H NMR (500 MHz, CD₃OD): δ 8.64 (*d*, *J* = 9.2 Hz, 1H), 8.60 (*d*, *J* = 9.2 Hz, 1H), 8.03 (*d*, *J* = 8.4 Hz, 2H), 7.82–7.34 (*m*, 11 H), 6.48 (*d*, *J* = 2.2 Hz, 1H), 4.70–4.37 (*m*, 4H), 4.30–4.13 (*m*, 2H), 2.88 (*s*, 2H), 2.78–2.67 (*m*, 4H), 1.88–1.72 (*m*, 6H), 1.41–1.16 (*m*, 6H) ppm; UV-vis (H₂O/CH₃CN/TFA = 40/60/0.05): λ_{\max} (relative intensities) 248 (86%), 292 (100%), 334 (48%) nm; IR: ν 3330 (br), 3360 (m), 2940 (m), 2870 (w), 2100 (s), 1730 (w), 1700 (w), 1590 (s), 1520 (w), 1490 (w), 1450 (m), 1370 (m), 1230 (m), 1160 (m), 1120 (w), 1060 (s), 950 (m), 830 (m) cm⁻¹; HRMS (ESI-TOF) calcd for C₄₂H₄₅N₈ (M⁺), 661.3767; found, 661.3756.

***anti*-TA2PZ5:** ¹H NMR (400 MHz, CD₃OD): δ 8.71–8.23 (*m*, 4H), 7.67–7.12 (*m*, 11 H), 6.45 (*d*, *J* = 2.2, 1H), 4.40–4.2 (*m*, 6H), 3.01 (*s*, 2H), 2.62 (*t*, *J* = 7.42 Hz, 2H), 1.95–1.72 (*m*, 6H), 1.38–1.20 (*m*, 6H) ppm; UV-vis (H₂O/CH₃CN/TFA = 40/60/0.05): λ_{\max} (relative intensities) 248 (95%), 292 (100%), 334 (51%) nm; IR: ν 3340 (br), 2940 (m), 2840 (w), 2100 (s), 1690 (w), 1590 (s), 1520 (w), 1480 (w), 1450 (m), 1350 (m), 1250 (m), 1180 (m), 1160 (m), 1040 (s), 950 (m), 830 (m) cm⁻¹; HRMS (ESI-TOF) calcd for C₄₁H₄₃N₈ (M⁺), 647.3611; found, 647.3596. Table 3 shows analytical HPLC conditions for selected compounds.

Determination of AChE–Inhibitor Association and Dissociation Rate Constants. The association rate constants (k_{on}) were determined by following the rate of quenching of the intrinsic AChE tryptophan fluorescence upon inhibitor binding using the stopped-flow technique.⁵¹ For femtomolar and low picomolar inhibitors, we determined the first-order dissociation rate constants (k_{off}) by measuring the return of AChE activity upon 5000-fold dilution of 50–100 nM concentrations of AChE–inhibitor complex into 250 μ g/mL solution of calf thymus DNA (USB Corp., Cleveland, OH) using the Ellman assay.⁵² The DNA sequesters the free phenanthridinium ion upon its release from the AChE complex through intercalation, thus preventing its reassociation with AChE when inhibitor concentrations in the reactivation medium are above their K_d . High picomolar inhibitors dissociated faster, and the reactivation medium contained no DNA, but substrate acetylthiocholine and thiol reagent DTNB were added to the reactivation medium for continuous monitoring of enzyme activity immediately upon dilution of AChE–inhibitor complex. The dissociation constants were determined by nonlinear fitting of the first-order increase in enzyme activity up to 100% of the AChE control activity in mixture containing no inhibitor. Alternatively, k_{off} values of fast dissociating inhibitors were determined using stopped-flow techniques, by following the partial return of intrinsic tryptophan fluorescence caused by dissociation of the AChE–inhibitor complex upon mixing with high concentration (100 μ M) of competing ligand (ambenonium or other tight binding ligand) to prevent inhibitor reassociation.

All experiments were performed in at least triplicate with the standard error of determination smaller than 20% of the mean value. The measurements were performed in 0.1 M phosphate buffer pH 7.0 at 22 °C on a SX.18 MV stopped-flow instrument (Applied Photophysics) or Cary 1E UV-vis spectrophotometer (Varian).

The equilibrium dissociation constants for the *syn*- and *anti*-TA2PZ6, TA2PZ5, and TZ2PA5 isomers, calculated as the ratios of their first-order dissociation and second-order association rate constants, are listed in Table 1, along with the dissociation constants for the TZ2PA6 isomers obtained previously.²⁴

(51) Radic, Z.; Taylor, P. *J. Biol. Chem.* **2001**, *276*, 4622–4633.

(52) Ellman, G. L.; Courtney, K. D.; Valentino Andres, J.; Featherstone, R. M. *Biochem. Pharmacol.* **1961**, *7*, 88–95.

Conclusions

We have optimized the in situ click chemistry approach to lead discovery and increased its scope using acetylcholinesterase as the target. The application of LC/MS–SIM for product identification greatly enhanced the sensitivity and reliability of the method and allowed the incubation times to be decreased from 6 days to as little as 6 h. Three new AChE inhibitors, in addition to the known compound, **TZ2PA6**, were identified from a library of tacrine and phenanthridinium azide and acetylene reagents, which contained the building blocks from previous work and the new **PZ5**.²⁴ All inhibitors, **TZ2PA6**, **TZ2PA5**, **TA2PZ6**, and **TA2PZ5**, were produced with almost complete selectivity for the *syn*-triazole isomer by both eel and mouse enzymes. This is a surprising discovery for **TZ2PA5** and **TA2PZ5**, in view of their reduced linker lengths. The *syn*-triazoles, formed by the enzyme, are more than 100 times more potent than the corresponding anti-isomers. Detailed binding studies revealed all in situ hit compounds to be extremely potent AChE inhibitors, with dissociation constants in the femtomolar range, due to the multivalent nature of the binding interactions, which also involve the newly formed *syn*-triazole heterocycle as an active pharmacophore.²⁵ The LC/MS–SIM technique enables the testing of multicomponent mixtures, thereby dramatically increasing the efficiency of the method and setting

the stage for medium- or even high-throughput screening. We are currently completing a search for novel and druglike AChE inhibitors based on this method and are investigating other enzyme and receptor targets, such as HIV protease, carbonic anhydrase, and nicotinic acetylcholine receptors.

Acknowledgment. We thank Professors M. G. Finn, V. V. Fokin, and Mr. W. G. Lewis for advice and helpful discussions. We are grateful to Professor G. Siuzdak and Mr. J. Apon for MALDI mass spectroscopy support. We also thank Dr. Luke Green for providing samples of azides and acetylenes used in initial experiments. This work was supported by the Swiss National Science Foundation and the Novartis Research Foundation (R.M.), by the Skaggs Foundation (H.C.K., A.K., R.M.), and the NIH (K.B.S. and P.T., Grants No. R-37GM18360 and DAMDC17C-02-2-0025 to P.T.).

Supporting Information Available: LC/MS–SIM traces for in situ click chemistry and control experiments, experimental details, LC/MS–SIM traces for regioisomer determination, and tables with free energy increments for structural modifications. This material is available free of charge via the Internet at <http://pubs.acs.org>.

JA046382G